Correction of the baseline fluctuations in the GEM-based ALICE TPC

ALICE TPC Collaboration

胡晓宇，黄启轩，葛景业

ALICE Run 3 TPC upgrade

- MWPC → GEM
- Readout: 3kHz→ 50kHz
- Triggered → continuous

Optimized to balance gain, ion backflow, energy resolution and stability

Continuous readout requires online calibration and correction before data compression.

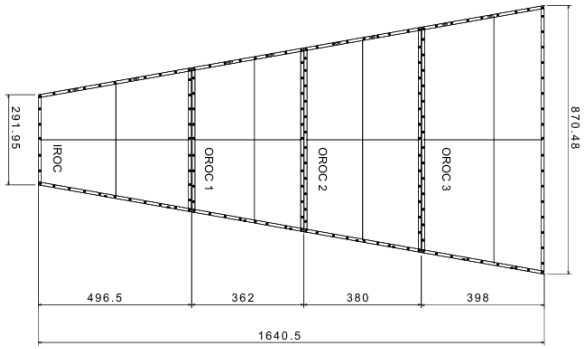

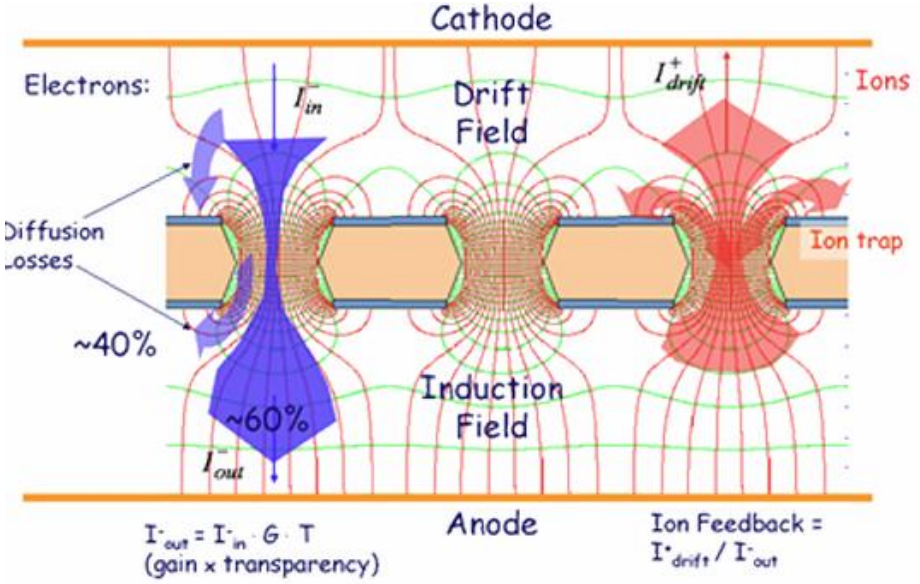

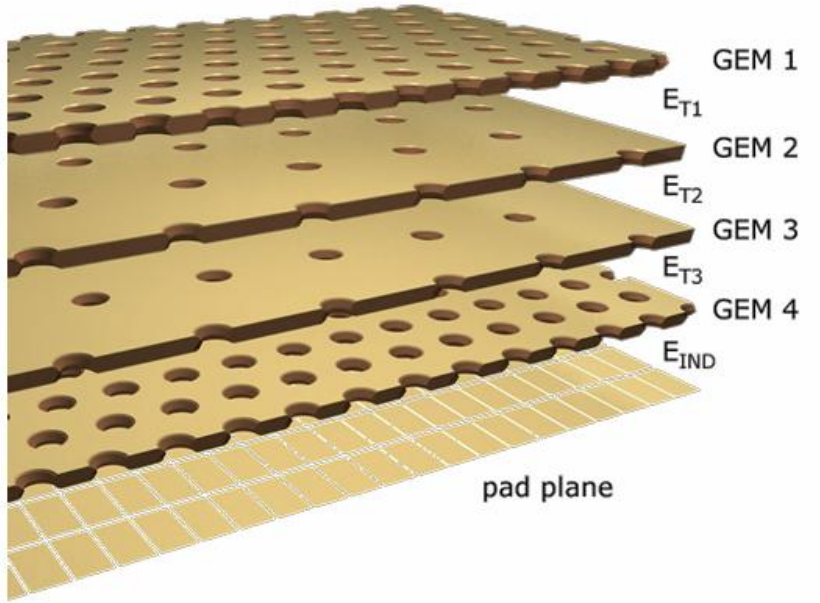

Calibration measurements: laser data

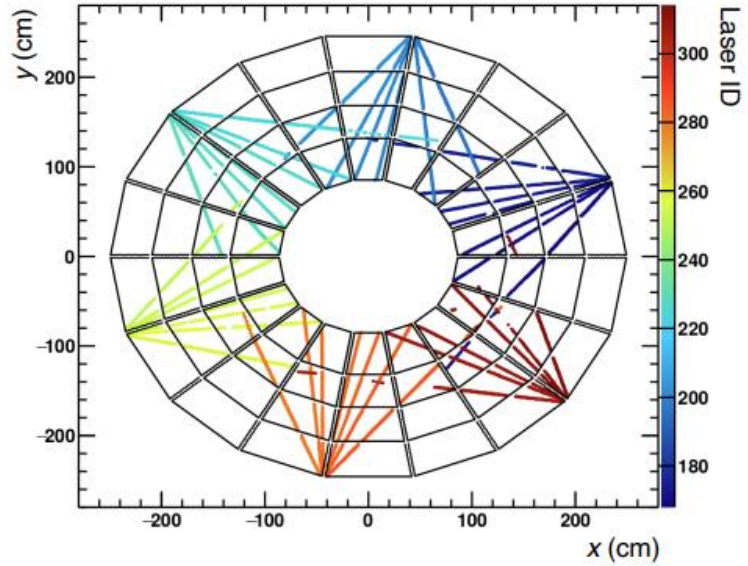

Laser wavelength: 266 nm （4.66eV); ionizes organic impurities via two-photon processes.
About 400–1200 laser events per sector were averaged to improve signal-to-noise ratio.

Two different effects to be corrected:
common-mode (CM) effect and ion tail (IT)

Laser data reveal two baseline effects:
• Common-mode undershoot on non-signal pads
• Positive ion tail after the main signal

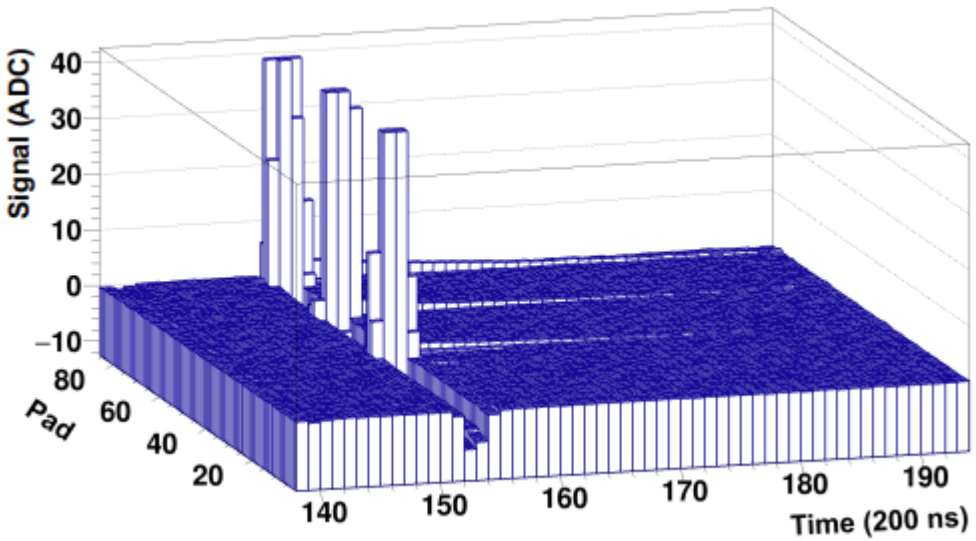

Calibration measurements: Calibration pulser data

- Pulse injected into GEM4B induces signals on the pad plane.
- Ideally, all pads in the same stack should measure the same charge.
- Pad-by-pad differences arise from local capacitance variations:
  – GEM foil sagging changes the pad–GEM distance.
  – Spacer crosses / edges contain dielectric material.

- Used as a pad-by-pad capacitance proxy for CM correction.

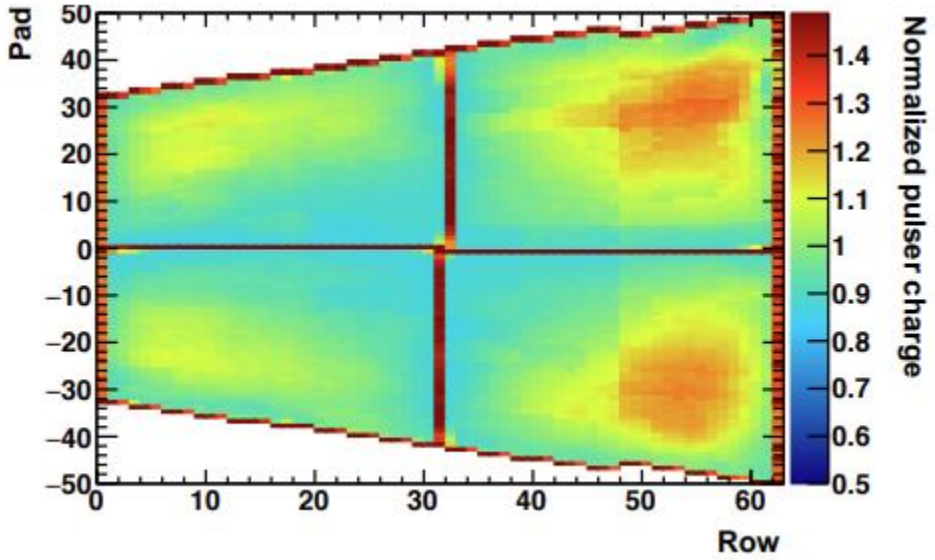

$$Q_{pulser,pad}^{norm} = \frac{\mathrm{Q_{pulser}}}{\mathrm{Q_{stack}^{median}}}$$

Ratio of pulser charge to median pulser charge in the stack for IROC.

Common-mode effect

The common-mode effect results from the capacitive coupling between the GEM foils and the pad plane.

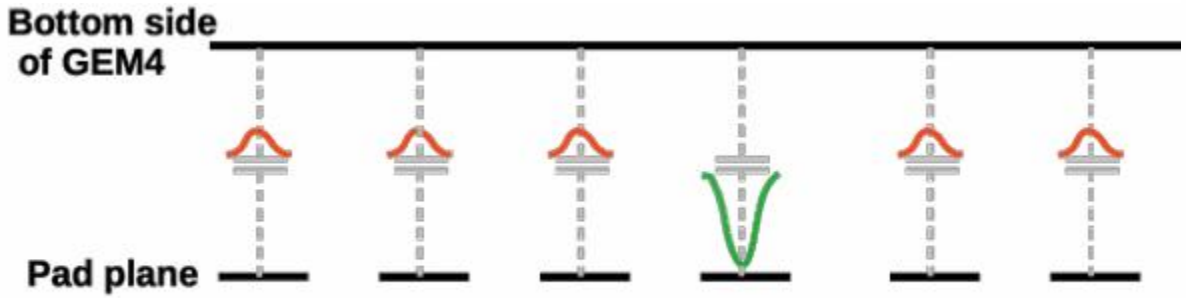

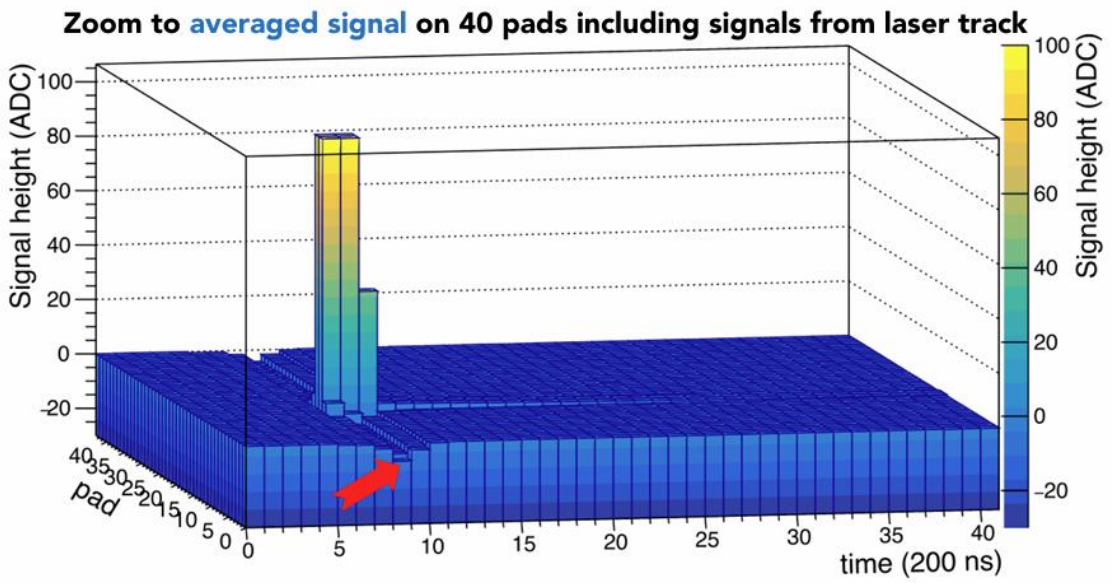

The magnitude of the undershoot in each pad for a given time bin, $Q_{pad}^{CM}(t)$, is proportional to the sum of the positive signal in the stack at the same time bin.

$$Q_{pad}^{CM}(t) \propto \sum_{\substack{Q(t)>0 \\ instack}} Q(t)$$

Common-mode fraction factor

$$k_{CF,pad} = \frac{Q_{pad}^{CM}(t)}{<Q_{pos}(t)>_{stack}},$$

where

$$< Q_{pos}(t) >_{stack} = \frac{\sum_{Q(t)>0} Q(t)}{instack \over N}$$

Common-mode effect

Random Forest (RF) machine learning algorithm to learn the dependencies of $k_{CF,pad}$

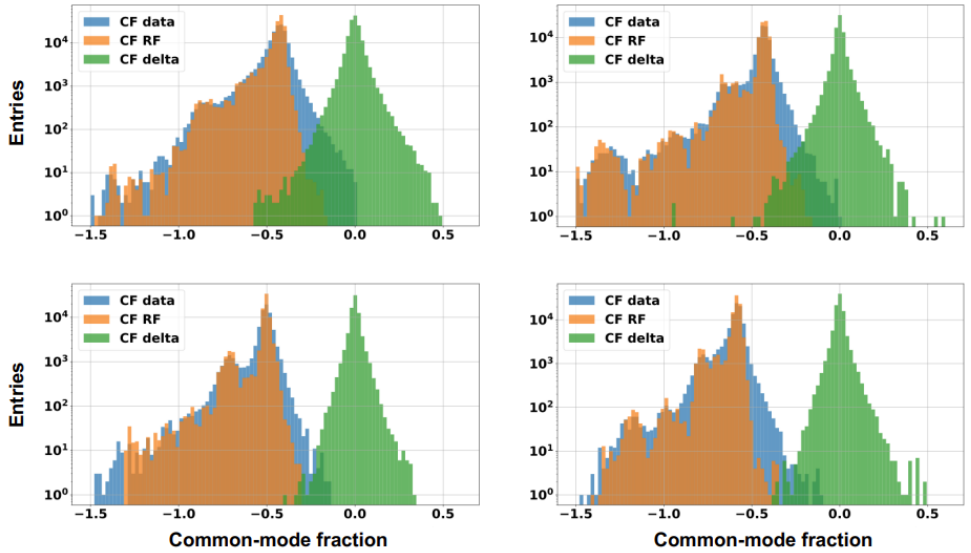

Variable	Variable importance (%)
normalized pulser charge ($Q^{\text{norm}}_{\text{pulser,pad}}$)	61.1
stack type	36.1
average positive signal in stack	1.0
fraction of signal pads in stack	0.8
remaining dependencies	1.0

	Stack area (mm^2)	Peak position of CF
IROC	171154	-0.42 ± 0.03
OROC1	174853	-0.43 ± 0.02
OROC2	231284	-0.50 ± 0.02
OROC3	294836	-0.58 ± 0.02

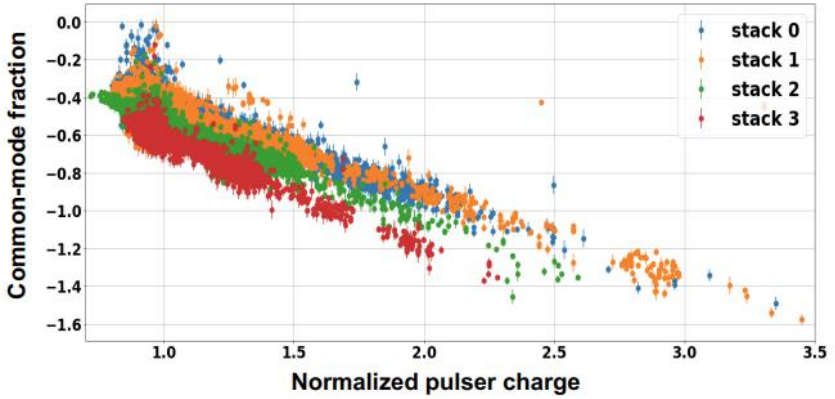

$$k_{\text{CF,pad}} = k_{\text{stack}} \cdot Q^{\text{norm}}_{\text{pulser,pad}}$$

CM online correction

- Each TPC stack is read out by multiple CRUs（over 3000 pads）:– OROC: 2 CRUs – IROC: 4 CRUs
- Since CRUs cannot exchange information online, the stack-level CM calculation cannot be applied directly.

$$k_{CF,pad} = \frac{Q_{pad}^{CM}(t)}{< Q_{pos}(t) >_{stack}}$$

$$k_{CF,pad} = k_{stack} \cdot Q_{pulser,pad}^{norm}$$

$$\rightarrow \qquad Q_{pad}^{CM}(t) = Q_{pulse,pad}^{norm} \left\langle \frac{Q_{pad}(t)}{Q_{pulse,pad}^{norm}} \right\rangle$$

where ⟨⟩ denotes averaging over empty pads in a given CRU.

$$\text{Candidate empty pad:} \qquad Q_{\text{pad}}(t) < Q_{\text{thr1}}$$

$$\text{Additional empty-pad check:} \qquad \left| \frac{Q_{\text{pad}}(t)}{k_{\text{pulser,pad}}} - \frac{Q_{\text{rndm}}(t)}{k_{\text{pulser,rndm}}} \right| < Q_{\text{thr2}}$$

$$N_{\text{padsOK}} > N_{\text{padsMin}} \quad \Rightarrow \quad \text{pad is selected as empty}$$

$$Q_{\text{baseline}}(t) = \left\langle \frac{Q_{\text{pad}}(t)}{k_{\text{pulser,pad}}} \right\rangle_{\text{empty pads}}$$

$$Q_{\text{pad}}^{\text{corr}}(t) = Q_{\text{pad}}(t) - k_{\text{pulser,pad}} \left\langle \frac{Q_{\text{pad}}(t)}{k_{\text{pulser,pad}}} \right\rangle_{\text{empty pads}}$$

Ion tail

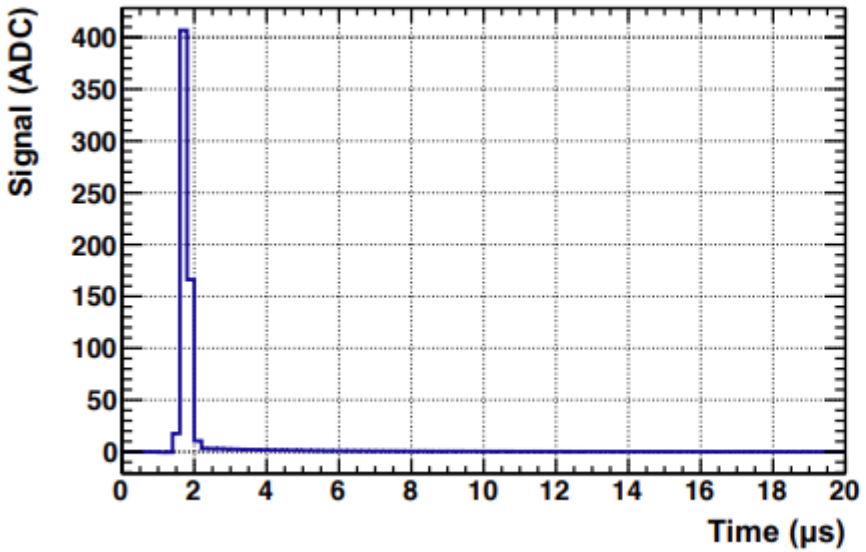

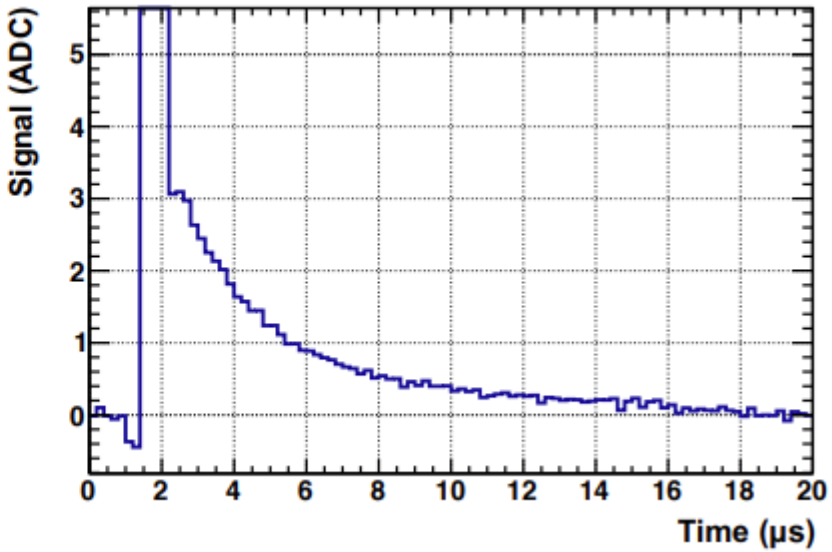

- The ion tail lasts about 16 μs after the signal peak.
- Peak amplitude: ~0.7% of the electron signal maximum.
- Integrated tail charge: ~9% of the total electron signal charge.
- Although small in amplitude, the accumulated tail charge is non-negligible.

The ion tail is caused by positive ions produced during GEM4B amplification.
While electrons are collected rapidly on the pads, ions drift slowly and induce a delayed signal, producing a long positive tail after the main pulse.

Ion tail parametrization

Ion-tail fraction: $f_{\mathrm{IT}} = \frac{Q_{\mathrm{tot}}^{\mathrm{tail}}}{Q_{\mathrm{tot}}^{\mathrm{signal}}}$

Ion-tail slope: $k_2 = e^{-\lambda_{\mathrm{IT}}}$

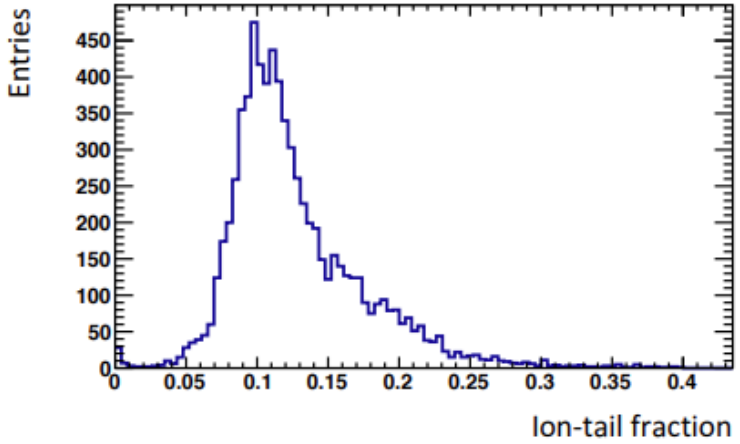

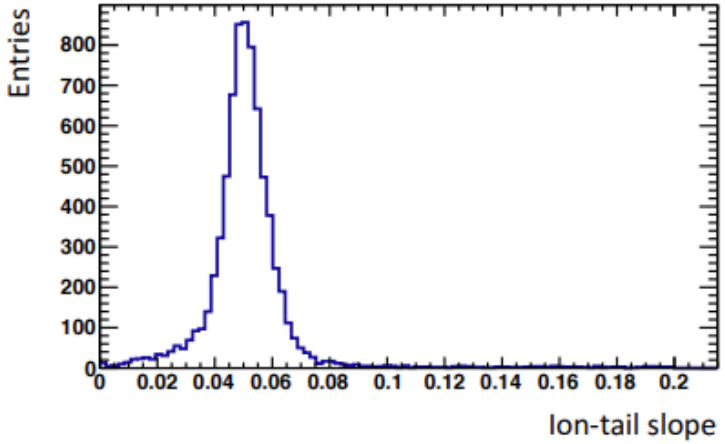

each pad signal was fitted with the convolution of a Gaussian and an exponential function to simultaneously describe the signal and tail

Ion tail online correction

the ion tail can be corrected online to first order and the remaining second-order deficiencies can be handled during track reconstruction.

$$Q_{\mathrm{out}}(t) = Q_{\mathrm{in}}(t) - \sum_i A_i \cdot e^{-\lambda_i (t - t_{\mathrm{i,max}})}$$

two problems: the number of resources required and the time needed to perform the calculations.

$$Q_{out}(t) = Q_{in}(t) - k_1(1 - k_2)Q_{corr}(t)$$
$$Q_{\mathrm{corr}}(t+1) = k_2[Q_{\mathrm{corr}}(t) + Q_{\mathrm{in}}(t)]$$
$$k_1 = k_0 f_{\mathrm{IT}}$$
$$k_2 = e^{-\lambda_{\mathrm{IT}}}$$
$$f_{\mathrm{IT}} = \frac{Q_{\mathrm{tot}}^{\mathrm{tail}}}{Q_{\mathrm{tot}}^{\mathrm{signal}}}$$

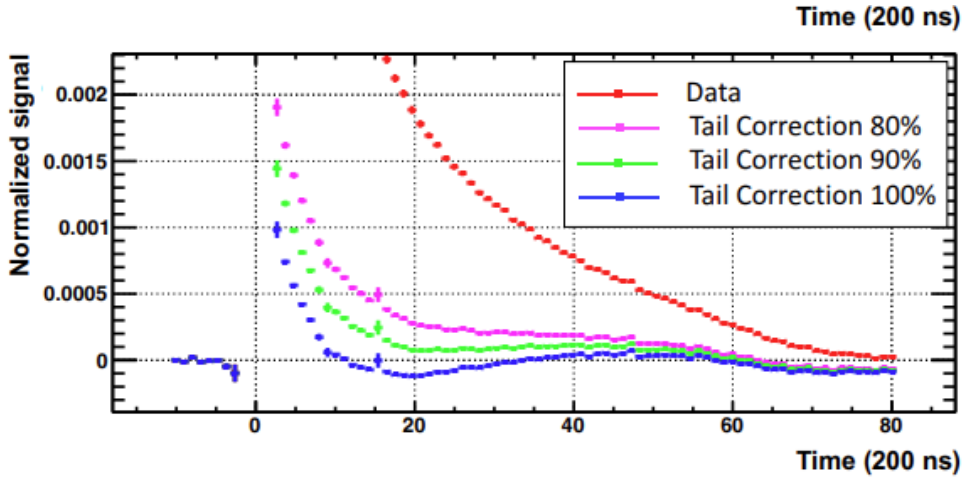

- Ion-tail correction also reduces the TPC data volume.

Performance(MC)

.

- Left panels: average baseline shift as a function of occupancy.
- Right panels: RMS of baseline fluctuations as a function of occupancy.

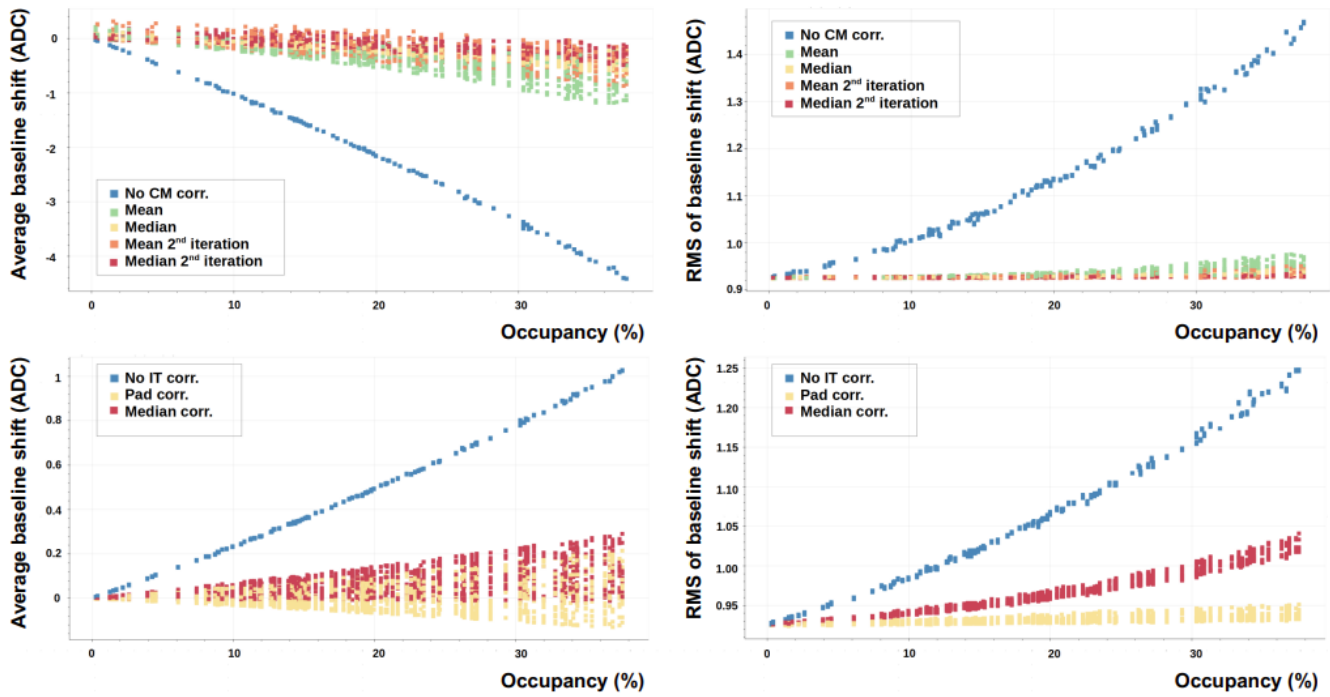

High occupancy in this study corresponds to about 30%, which is close to the expected highest Run 3 Pb–Pb multiplicity conditions.

$$space\ saving(\%) = 100\% - \frac{compressed\ data\ size}{uncompressed\ data\ size}$$

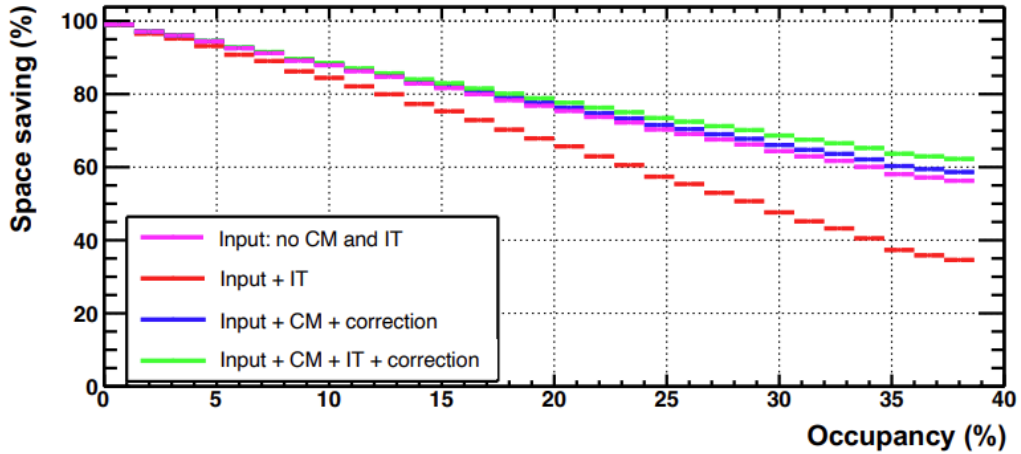

Minimum bias PbPb events, occupancy < 30%	Minimum bias space saving (%)	GB/s
input signal	81.4	650
input + ion tail	74.6	888
input + common-mode + correction	82.1	628
input + ion tail + common-mode + correction	83.1	594
current assumption	82.9	600

Summary and outlook

- Laser and pulser calibration data were used to study common-mode and ion-tail effects.
- Common-mode correction is based on local capacitance variations, described by normalized pulser charge.
- Ion-tail correction uses calibrated tail fraction and slope parameters in an exponential filter.
- Toy MC validation shows that both algorithms efficiently recover the baseline bias and RMS fluctuations.
- Correcting the ion tail is also crucial for data compression, reducing the rate back toward the expected ~600 GB/s scale.

- The two correction algorithms have been commissioned as part of the TPC readout system from 2023 onward.
- Future studies with full MC and collision data are needed to evaluate residual biases and track-topology effects.

Back up(slide 3)

Very large signals saturating the dynamic range of the SAMPA chip were discarded from the analysis, since their actual amplitude is not known. Moreover, very large charges fed into the input of the SAMPA chip may lead to loss of sensitivity of this channel for a short time. This can be seen as a saturation of the SAMPA response at a constant value of about 100 ADC, as shown in the right panel of Fig. 5 with red and brown solid lines. Note that this effect is an artifact of the electronics and therefore does not affect the neighboring pads.

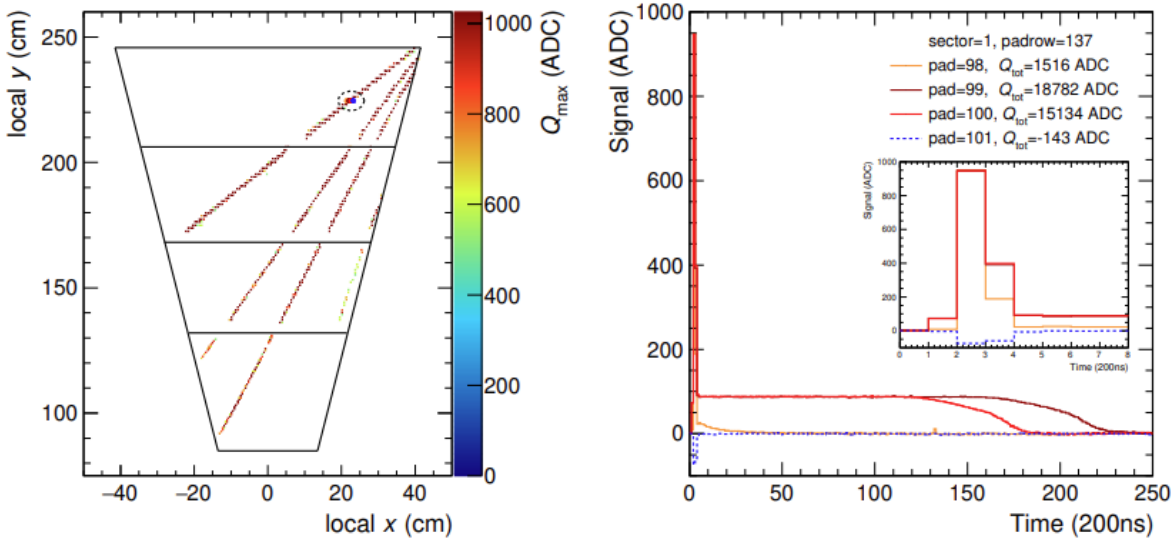

Figure 5: Left: four laser tracks projected on to the local x–y plane. The dashed oval highlights saturated signals. Right: saturated laser signals of the cluster highlighted in the left panel.

Ion tail

Simulation for two types of ions that contribute to the ion tail:
GEM hole
Induction gap $E_{ind}^{100\%} = 3.5\text{kV/cm}$

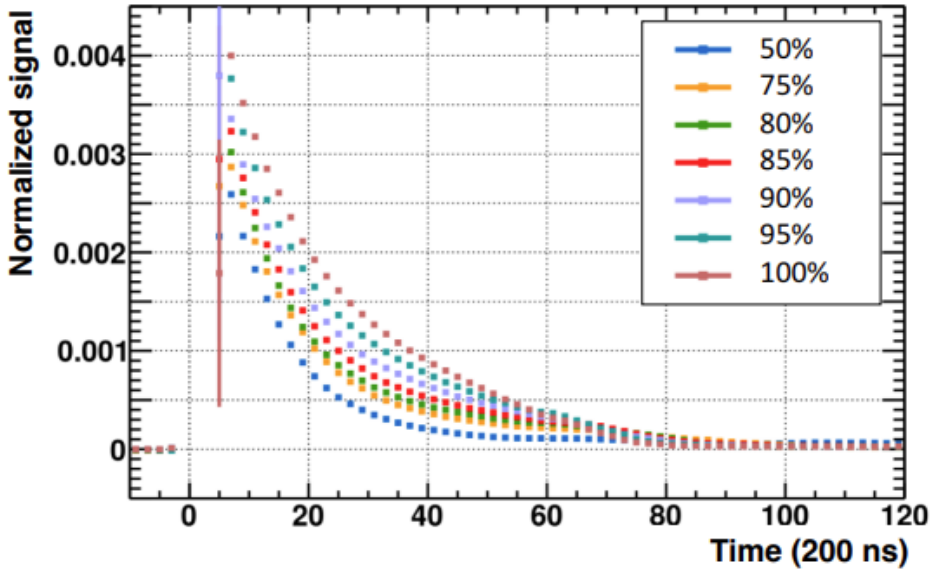

$$Q_{\text{fast}}(E_{\text{ind}}) \approx Q_{\text{meas}}(E_{\text{ind}}^{50\%})$$

$$Q_{\text{slow}}(E_{\text{ind}}) \approx Q_{\text{meas}}(E_{\text{ind}}) - Q_{\text{meas}}(E_{\text{ind}}^{50\%}).$$

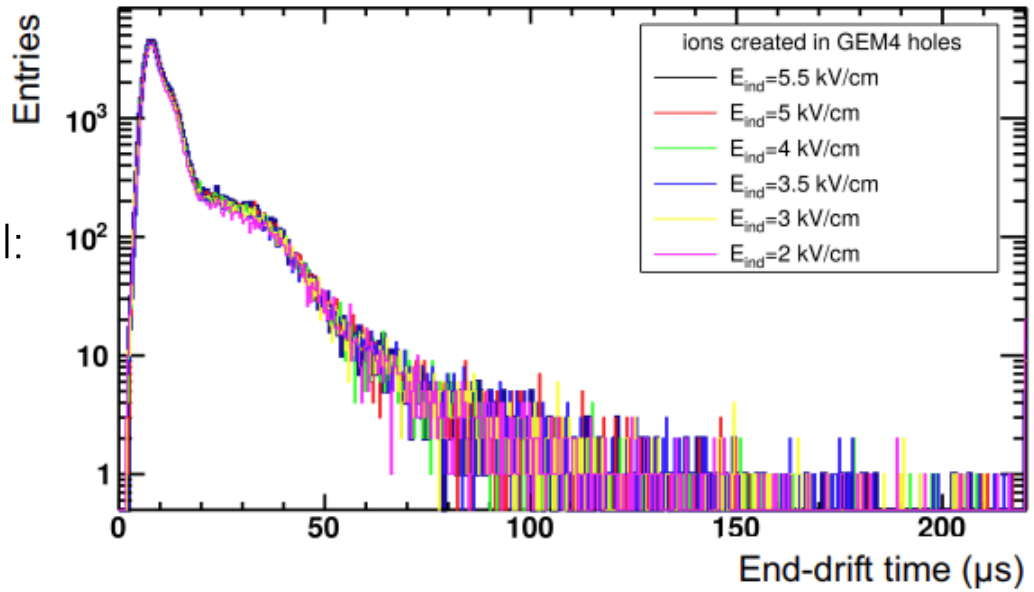

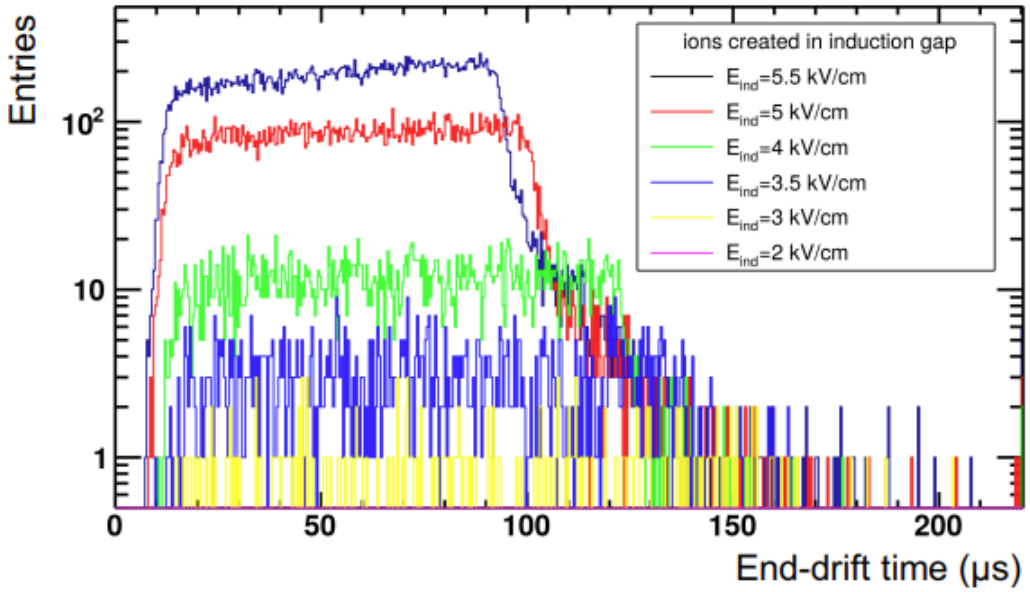

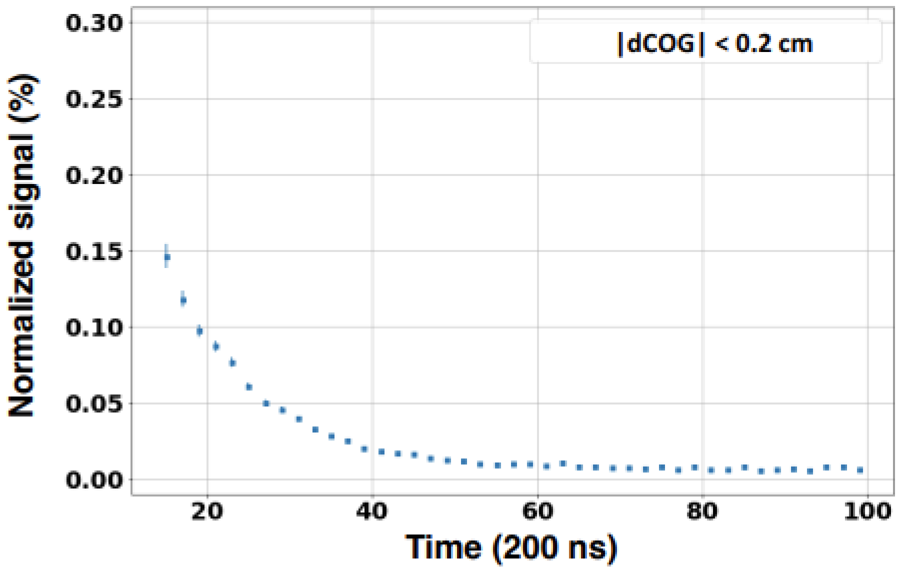

- Left: ion tail measured at 50% induction field.
- Right: ion tails at 100%, 85%, and 75% induction field.
- The slow component is nearly linear in time and decreases as the induction field is reduced.
- Only central pads of OROC3 are shown.

The ion tail can be corrected online using an exponential filter algorithm. However, the additional linear component must be taken into account to avoid any bias.

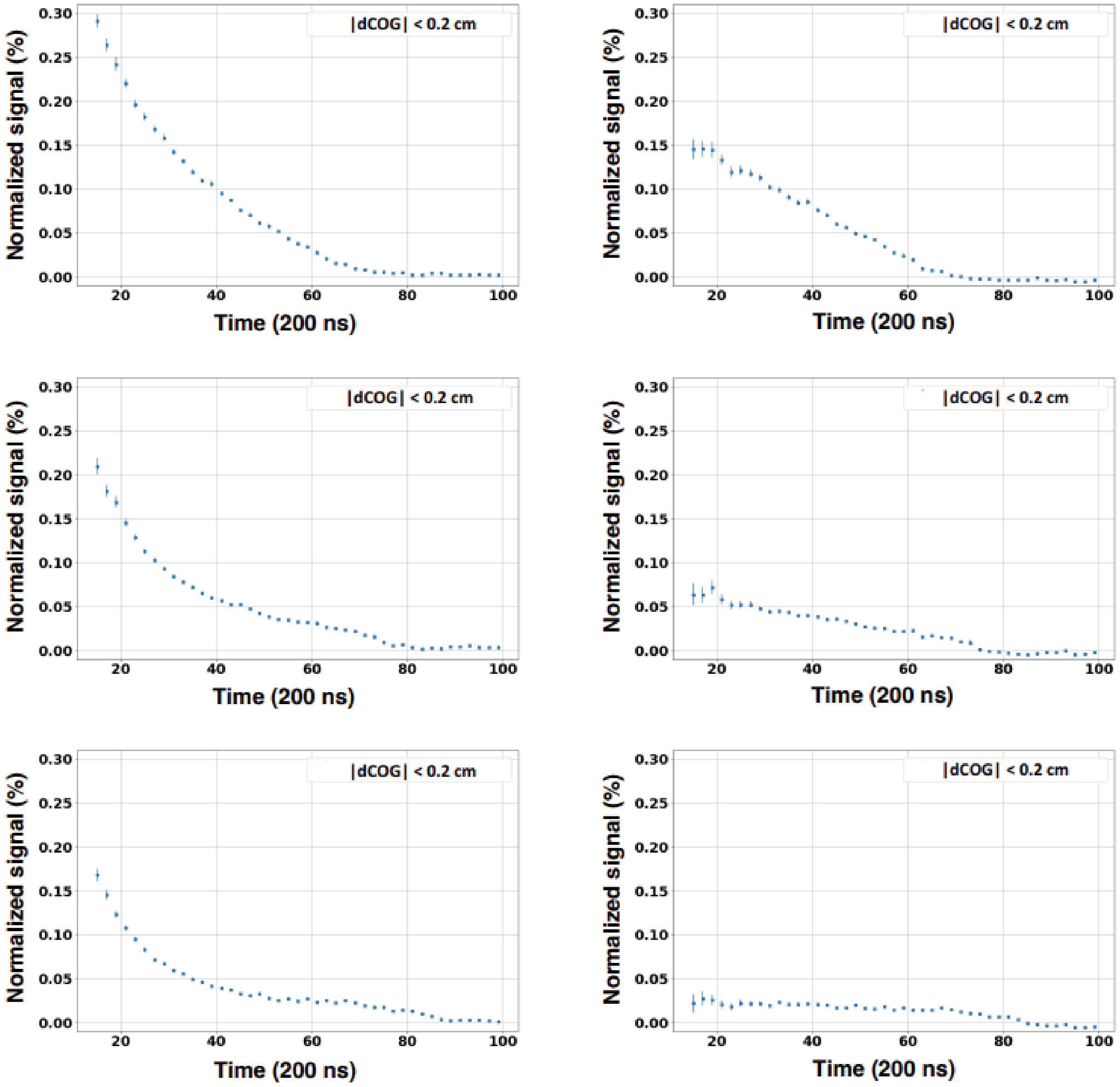

Ion tail parametrization

ion-tail fraction $f_{IT}(\mathrm{E_{ind}}) = \frac{Q_{tot}(tail)}{Q_{tot}(signal)}$

$$f_{\mathrm{IT}}(E_{\mathrm{ind}}) = A + B \cdot e^{C \cdot E_{\mathrm{ind}}}$$

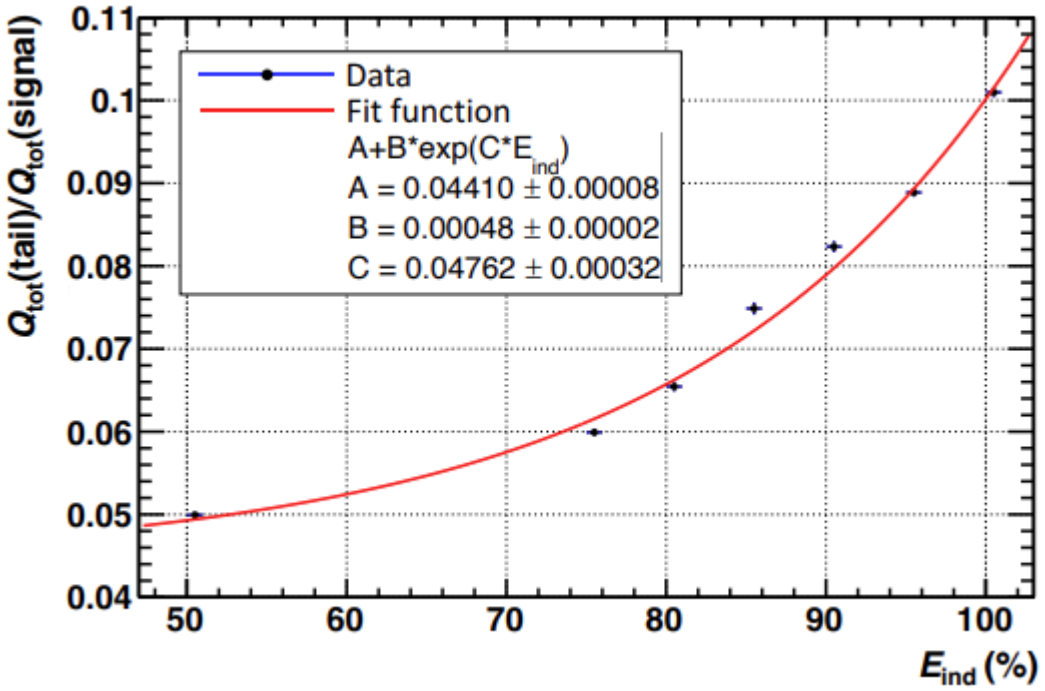

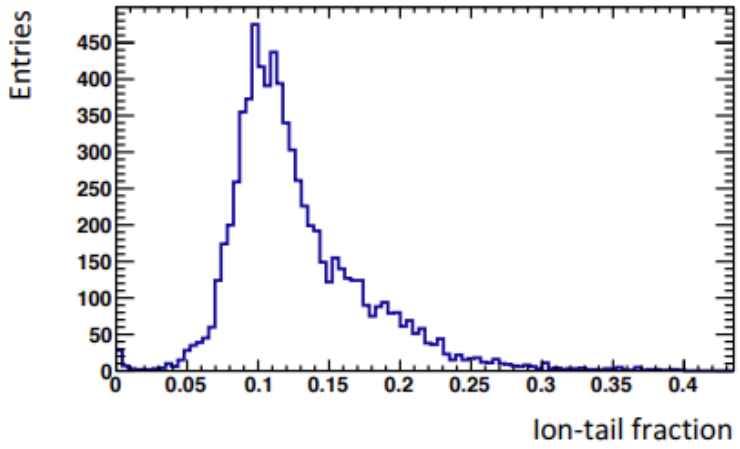

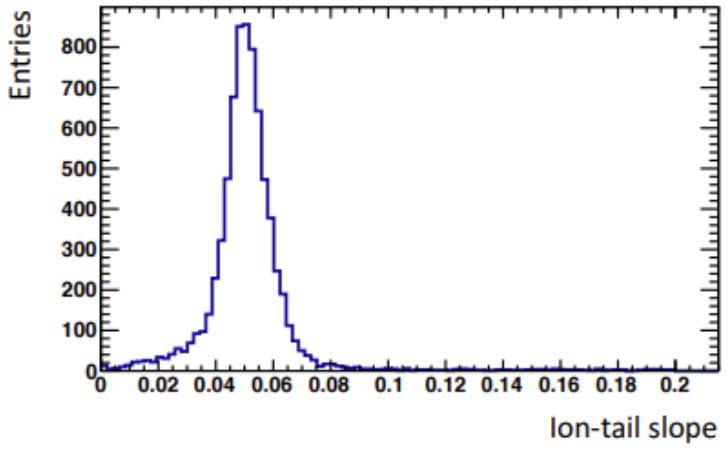

each pad signal was fitted with the convolution of a Gaussian and an exponential function to simultaneously describe the signal and tail

Back up slide(9)

为了理解 GEM 中观测到的 ion tail 的起源，研究人员进行了模拟。

在这些模拟中，只建模了最后一层 GEM 箔片，也就是 **GEM4**。作为一阶近似，这是足够的，因为 GEM4 电极会屏蔽前面放大阶段中产生的离子。

电场图使用有限元方法计算，该方法在 **ANSYS** 中实现。电荷载流子的输运性质使用 **Magboltz** 计算，其倍增过程使用 **Garfield++** 模拟。

模拟显示，有两类离子会对 ion tail 有贡献。它们可以按照产生位置来分类：

1. 在 **GEM4 holes** 中产生的离子；
2. 在 **induction gap** 中产生的离子，也就是 GEM4B 与 pad plane 之间区域产生的离子。

Backup common-mode

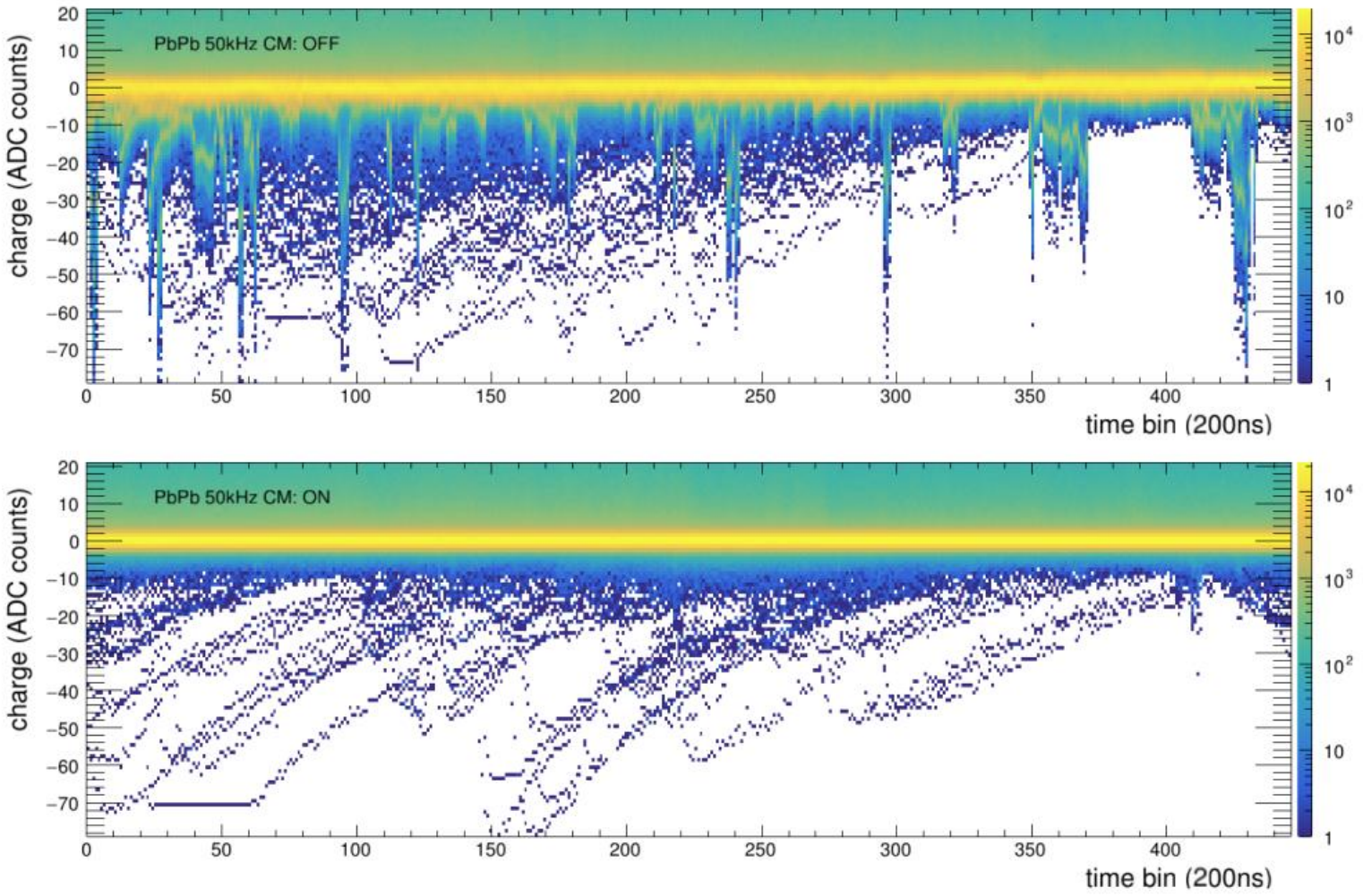

CRU 中的负向 common-mode baseline excursions 被显著抑制。

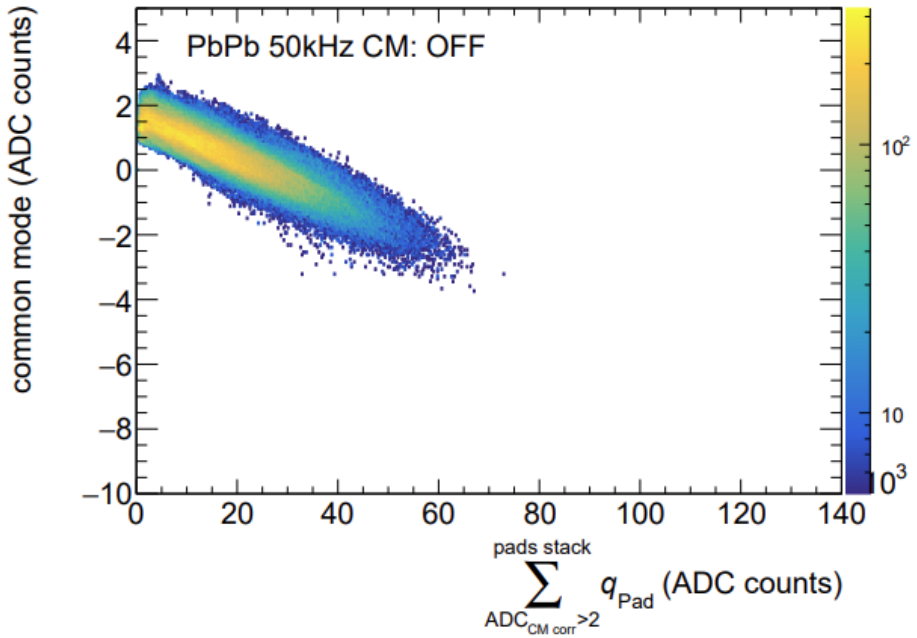

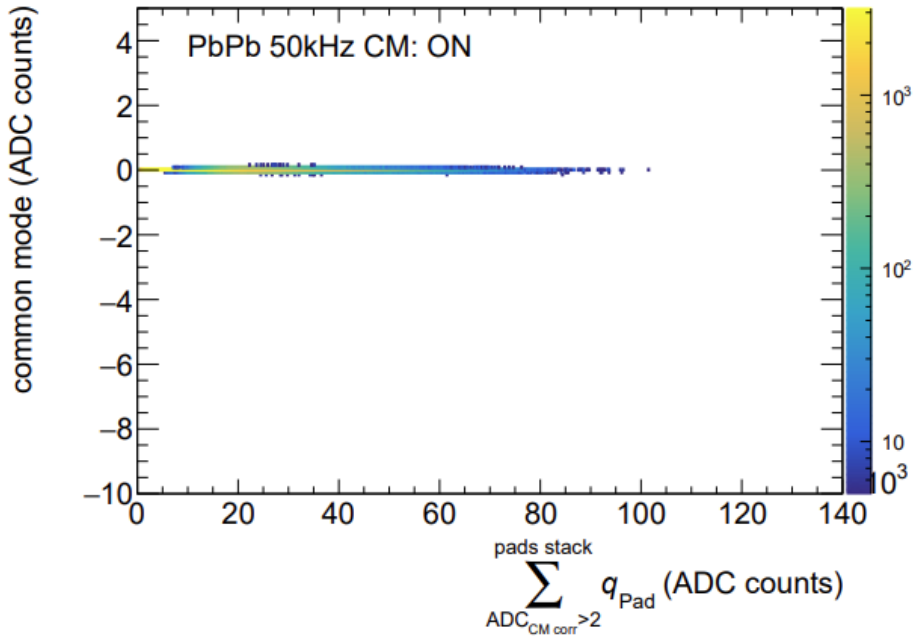

消除了正信号强度与 common-mode 偏移之间的相关性

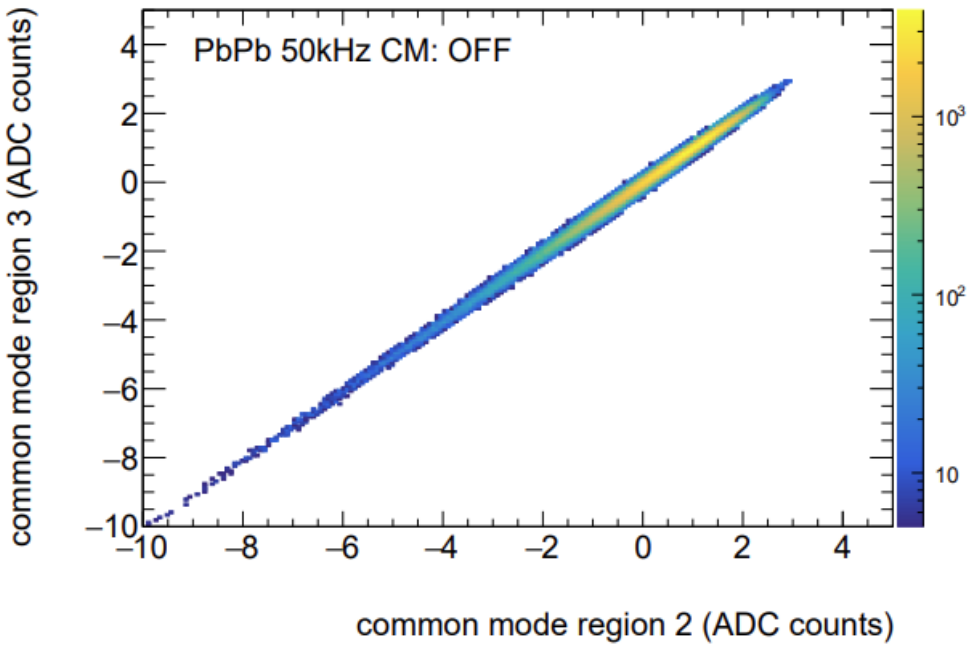

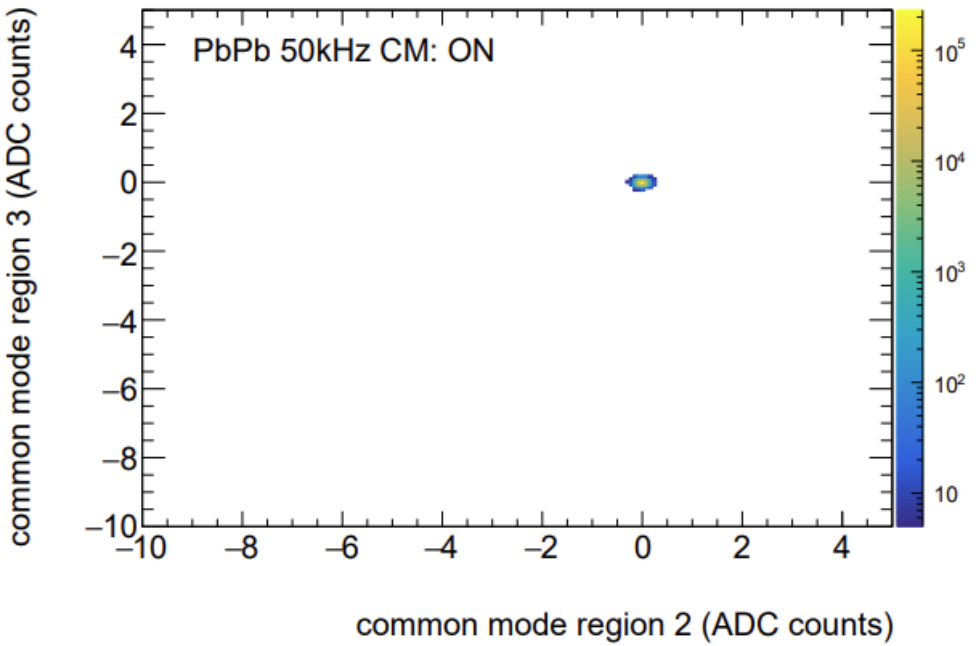

即使同一个 GEM stack 被多个 CRU 分区读出，CRU-based common-mode correction 仍然能独立、稳定地去除 common-mode。